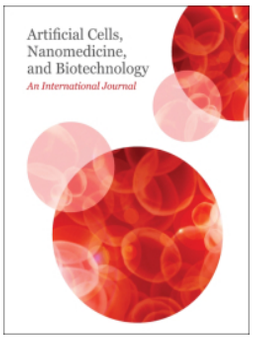

Taylor & Francis
Taylor & Francis Group

Artificial Cells, Nanomedicine, and Biotechnology
An International Journal

ISSN: (Print) (Online) Journal homepage: www.tandfonline.com/journals/ianb20

# Green synthesis, characterisation and antibacterial activities of *Strobilanthes crispus*-mediated silver nanoparticles (SC-AGNPS) against selected bacteria

**Rohazila Mohamad Hanafiah, Siti Aisyah Abd Ghafar, Vuanghao Lim, Siti Nor Asma Musa, Fahmi Yakop & Arif Haikal Hairil Anuar**

**To cite this article:** Rohazila Mohamad Hanafiah, Siti Aisyah Abd Ghafar, Vuanghao Lim, Siti Nor Asma Musa, Fahmi Yakop & Arif Haikal Hairil Anuar (2023) Green synthesis, characterisation and antibacterial activities of *Strobilanthes crispus*-mediated silver nanoparticles (SC-AGNPS) against selected bacteria, Artificial Cells, Nanomedicine, and Biotechnology, 51:1, 549-559, DOI: 10.1080/21691401.2023.2268167

**To link to this article:** https://doi.org/10.1080/21691401.2023.2268167



Published online: 17 Oct 2023.

ARTIFICIAL CELLS, NANOMEDICINE, AND BIOTECHNOLOGY
2023, VOL. 51, NO. 1, 549–559
https://doi.org/10.1080/21691401.2023.2268167



# Green synthesis, characterisation and antibacterial activities of *Strobilanthes crispus*-mediated silver nanoparticles (SC-AGNPS) against selected bacteria

Rohazila Mohamad Hanafiah[a], Siti Aisyah Abd Ghafar[a], Vuanghao Lim[b], Siti Nor Asma Musa[a,c], Fahmi Yakop[a] and Arif Haikal Hairil Anuar[a]

[a]Department of Basic Science, Faculty of Dentistry, Universiti Sains Islam Malaysia, Ampang Kuala Lumpur, Malaysia; [b]Integrative Medicine Cluster, Advanced Medical and Dental Institute, Universiti Sains Malaysia, Bertam, Kepala Batas, Penang, Malaysia; [c]Faculty of Science and Engineering, School of Pharmacy, University Nottingham Malaysia, Semenyih, Selangor, Malaysia

**ABSTRACT**

This study aims to characterize and determine the antibacterial activities of synthesized *Strobilanthes crispus*-mediated AgNPs (SC-AgNPs) against *Streptococcus mutans*, *Escherichia coli* and *Pseudomonas aeruginosa*. *S. crispus* water extract acts as a reducing and capping agent in the synthesis of AgNPs. The synthesized AgNPs were characterized by using UV-Vis spectrophotometer, dynamic light scattering (DLS), field emission scanning electron microscope (FESEM), X-ray diffractometer (XRD) and Fourier transform infra-red (FTIR). FESEM images showed a rough surface with a spherical shape. The average size distribution of 75.25 nm with a polydispersity index (PDI) of 0.373. XRD analysis matched the face-centred cubic structure of silver. FTIR analysis revealed a shifted peak from 1404.99 to 1345.00 $cm^{-1}$. MIC and MBC values of SC-AgNPs were 1.25 mg/mL and 2.5 mg/mL against *E. coli*, *P. aeruginosa and S. mutans*, respectively. Time-kill assay showed that SC-AgNPs significantly reduced bacterial growth as compared to non-treated bacteria. Morphologies of bacteria treated with SC-AgNPs were shrunk, lysed, irregular and smaller as compared to control. SC-AgNPs significantly disrupted the gene expression of *eae* A, *gtf* B and *Pel* A ($p < 0.05$). This study indicated that the synthesized SC-AgNPs were stable with enhanced antibacterial activities.

**ARTICLE HISTORY**
Received 11 November 2022
Revised 29 September 2023
Accepted 4 October 2023

**KEYWORDS**
Silver nanoparticles; *Strobilanthes crispus*; antibacterial; *Streptococcus mutans*; *Escherichia coli*; *Pseudomonas aeruginosa*

## Introduction

Novel utilization of nanoparticles and nanomaterials is developing on different fronts due to their new or improved properties dependent on size, distribution and morphology [1,2]. It is quickly acquiring redesign in many fields, for example, medical care, beauty care products, biomedical, drug-quality conveyance, climate, synthetic enterprises, gadgets and photograph electrochemical applications [3]. Silver nanoparticles (AgNPs) are becoming one of the fastest-growing product categories in the nanotechnology industry. This is attributed to their good electrical conductivity, chemical stability, catalytic and remarkably strong anti-microbial properties [4]. A wide category of products in this respect has already been available on the market. In the medical arena, there are wound dressings, scaffolds, contraceptive devices, dental materials, surgical instruments and bone prostheses that are coated or embedded with nanosilver [3,5].

A substantial amount of existing research has discussed the creation of silver nanoparticles using living organisms like bacteria, fungi, and plants. This is mainly due to their natural ability to reduce metal compounds into nanoparticles, thanks to their antioxidant or reduction properties. However, among the various ways to create silver nanoparticles using living organisms, the approach involving microorganisms isn't practically feasible for industries due to the demanding need for sterile conditions and their continuous management. Therefore, using plant extracts for this purpose holds promise as a better alternative to microorganisms. This is because it offers advantages such as easier enhancement, lower biohazard risk, and a simpler process for maintaining cell cultures [5]s. The synthesis of nanoparticles using plants is widely gaining interest among researchers. Therefore, green synthesis or bio-synthetics of nanoparticles especially using plants is becoming preferable among researchers as it was reported as clean, non-toxic and environmentally acceptable. Green synthesis method is the most popular method to synthesize nanoparticles. This technique used plant-based products as reducing agents due to the bioactive compound found in plants such as phenolic compounds [7]. The recent synthesis of green AgNP utilizes plant extracts such as *Azadirachta indica* [8], *Holarrhena antidysenterica* [9,10], *Piper longum* [11], *Arnebia hispidissima* [12], and many more. Plants extracts act as reducing agents for the synthesis of the nanoparticles and

CONTACT Siti Aisyah Abd Ghafar aisyahghafar@usim.edu.my Department of Basic Science, Faculty of Dentistry, Universiti Sains Islam Malaysia, Ampang Kuala Lumpur, Malaysia

they give more advantages as they are easily scaled up and less biohazard.

Other than acting as reduction and capping agents, bioactive such as phenolic compounds bind to AgNP and may enhance its medicinal properties. Several studies reported that phenolic compounds of the extract may enhance the medicinal properties of silver nanoparticles [13,14] For example, *Clinacanthus nutans* which were reported as reducing and capping agents of AgNPs showed better inhibition on cell cancer growth when compared to commercial silver nanoparticles [14]. Green synthesized AgNP exhibits antimicrobial properties by inhibiting bacteria growth and showing bacteriostatic and bactericidal ability against pathogenic bacteria [15]. Thus, it is essential to develop AgNP products based on a green approach without using hazardous substances to human health and the environment.

*Strobilanthes crispus* (*S. crispus*) is a medicinal plant that can be used to treat diabetes, diuretics, cancer and constipation [16]. In Malaysia, this plant also known as pecah beling, pecah kaca or bayam karang. *S. crispus* has been reported as an antioxidant, anti-angiogenic and wound healing agent. Koay et al. [17] reported that *S. crispus* alcoholic extracts exhibited antibacterial activities against selected pathogens such as *Bacillus subtilis*, *Staphylococcus aureus* and *Salmonella typhi*. *S. crispus* ethanolic leaf extracts have antibacterial activities towards *Pseudomonas aeruginosa*, *Escherichia coli* and *Candida albicans* [18]. However, report on antibacterial activities exposed to AgNP incorporated with *S. crispus* water extract is very limited. To date, this is the first study highlighting the synthesis of *S. crispus* mediated-AgNPs. Hence, this study aims to characterize and investigate the antibacterial activities of synthesized *S. crispus* mediated-AgNPs (SC-AgNPs) against selected bacteria.

## Materials and methods

### *Preparation of* Strobilanthes crispus *water extract*

*Strobilanthes crispus* was collected at TKC Herbal Ampangan, Seremban, Malaysia [Figure 1(a)]. *S. crispus* leaves were cleaned, separated and oven-dried at 45 °C. The leaves were ground into a fine powder and soaked in distilled water at room temperature. Water extracts were collected in clean glass bottles and filtered using Whatman no 1 filter paper. The water filtrate was then freeze-dried (Martin Christ, Germany). *S. crispus* water extract was kept at −20 °C until further use [14].

### *Synthesis of SC-AgNPs*

SC-AgNPs synthesis method was adapted from Yakop et al., [19]. Briefly, A total of 1 mM of silver nitrate was mixed with *S. crispus* leaves water extract at 4.5 mg/mL and incubated at room temperature for 24 h. Changes of colour to reddish brown which indicated the formation of AgNP were observed. SC-AgNPs were washed and freeze-dried to form a powder. Then, SC-AgNPs were kept at −20 °C until further use.

### *Characterization of SC-AgNPs*

The presence of SC-AgNPs was observed by gauging the reduction of silver ions by using UV–vis spectrophotometer (Shimadzu, Kyoto Japan) at the wavelength range of 250–800 nm [19]. The sample was diluted with ultrapure water at 1:1 volume before the measurement. Wheras the particle size, zeta potential, and polydispersity index (PDI) of SC-AgNPs were measured at room temperature by using a Zetasizer analyzer (Malvern Zetasizer Nano ZS; Nano-ZS90, Malvern, UK). The sample was diluted with ultrapure water at a 1:10 ratio and tested until the smallest size of SC-AgNPs was obtained. Parameters such as the refractive index of water (1.330), viscosity (0.8872 cP), and temperature (25 °C) were set before the analysis. For the surface morphology study sample was analyzed by using a field emission scanning electron microscope (FESEM) (JEOL JSM 7600 F, Japan). Thin films of AgNPs were placed onto a carbon-coated copper grid, and then, the films on the FESEM grid were allowed to dry for analysis. X-ray diffractometer (XRD) was used to

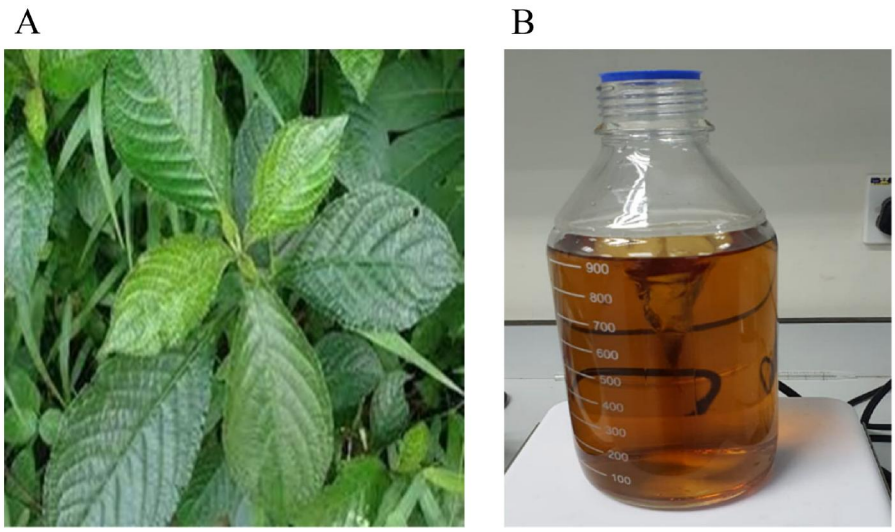


**Figure 1.** (A) *Strobilanthes crispus* leaves that were used in the study; (B) biosynthesis of AgNP mediated with *S. crispus* at 24h.

identify the crystallinity phase of silver in the sample by referring to the silver database from the Joint Committee on Powder Diffraction Standard (JCPDS) [20]. The sample was placed on a glass sample plate holder by flattening and compressing with an XRD machine (Rigaku Miniflex 600, Japan). The holder was mounted onto standard sample stages in the sample chamber. The X-ray wave was beamed, and the scattered intensity was measured. Fourier Transform Infra-red (FTIR) analysis was conducted using a Thermo Scientific™ Nicolet™ iS50 FTIR Spectrometer (Waltham, MA, USA) to observe the presence of functional groups in the sample. The sample was placed on a diamond crystal and touched with an ATR touch-point probe.

### Antibacterial activities SC-AgNPs against selected bacteria

Antibacterial activities of SC-AgNPs against *Escherichia coli* (Clinical strain-Department Bioscience, Nottingham University Malaysia), *Pseudomonas aeruginosa* (ATCC 10145) and *Streptococcus mutans* (ATCC 25175) were done by using disc diffusion assay, minimum inhibition concentration, minimum bactericidal concentration and time-kill assay.

### Bacteria preparation

*Escherichia coli* and *P. aeruginosa* were grown in brain heart infusion broth BHIB, (Oxoid, United Kingdom) for 24 h at 37 °C. Meanwhile, *S. mutans* were grown in BHIB for 24 h at 37 °C under facultative anaerobic conditions.

### Disc diffusion assay

The disc diffusion method was followed the method from Salehuddin et al. [21] and Lu et al [22], with modification. All the bacteria (*E. coli, P. aeruginosa and S. mutans*) were grown in Muller Hinton broth (MHB) (Oxoid, United Kingdom) and incubated for 24 h. After that, the turbidity of those bacteria was adjusted to 0.5 McFarland. A sterile cotton swab was dipped into the suspension and then spread evenly on Muller Hinton agar (MHA) to get consistent microbial growth. Sterilized filter paper discs with a size of 6 mm were impregnated with 5 μL of each SC-AgNPs, AgNP and *S. crispus* water extract at 10 mg/mL and placed on MHA. Gentamicin (10 μg) (Sigma-Aldrich, United States) was used as a positive control. All agar plates were incubated at 37 °C for 24 h and under aerobic conditions for *E. coli* and *P. aeruginosa*. Meanwhile, *S. mutans* were grown under facultative anaerobic conditions. After the incubation period, the inhibition zone was measured using a caliper.

### Minimum inhibition concentration (MIC) and minimum bactericidal concentration (MBC)

MIC and MBC methods were done by following the method from Salehuddin et al. [20] and Lu et al. [22], with modifications. All bacteria (*E. coli, P. aeruginosa and S. mutans*) were grown in Muller Hinton broth (MHB) (Oxoid, United Kingdom) and incubated for 24 h. After that, the turbidity of those bacteria was adjusted to 0.5 McFarland. Then, 100 μL of the bacteria were transferred to a 96-well plate. A total of 100 μL of SC-AgNPs, AgNP and *S. crispus* water extract with different concentrations were added to the well and the final volume for each well was 200 μL. After that, the cultured were incubated at 37 °C for 24 h. Colour changes were assessed visually after 50 μL of 3-(4,5-dimethylthiazol-2-yl)-2,5-diphenyltetrazolium bromide) tetrazolium (MTT) (Sigma-Aldrich, United States) was added. MBC is the continuous method from MIC. A volume of 5 μL of samples from the 96-well plate was cultured onto MHA and incubated at 37 °C for 24 h. After the incubation, the lowest concentration that inhibits bacterial growth was determined as MBC values.

### Time kill assay

Time kill assay was performed according to Hanafiah et al.[23] with slight modification. A single colony of test bacteria was inoculated in 10 ml MHB and incubated at 37 °C while shaking at 200 rpm overnight. The next day, these overnight bacterial cultures were used to prepare 10 ml of bacteria dilution at $1 \times 10^8$ CFU/mL using fresh Muller Hinton (MH) (Oxoid, United Kingdom) broth. About 100 μL of these diluted bacteria cultures were aliquot into 96 well plates and were added with 100 μL of SC-AgNPs (1/2 MIC, MIC and MBC), *S. crispus* water extract (10 mg/mL) and commercial AgNP (10 mg/mL). Gentamicin (MBC) was used as a positive control. Non-treated bacteria were used as inoculum controls respectively. *Pseudomonas aeruginosa* and *E. coli* plates were incubated under aerobic conditions while *S. mutans* plates were incubated under the anaerobic condition at 37 °C for a cumulative period of 24 h. A total of 20 μL cultures were collected from each well at 5 sampling points (T0 immediately after the addition of respective treatments, T4, T8, T12, and T24) throughout the 24h incubation period. Collected samples were diluted to tenfold dilution for another three times with 0.9% sodium chloride (NaCl) (Sigma-Aldrich, United States) solution, followed by spreading 10ul of each dilution onto MH agar plates. These agar plates were incubated at 37 °C for 24h and colonies on the plates had been counted and recorded as log CFU/mL.

### Scanning electron microscopic

Morphological changes of *S. mutans, E. coli and P. aeruginosa* by SC-AgNPs were observed with a scanning electron microscope (SEM) following the method by Goldbeck et al. [24] . Three treatment incubation times were tested which were 0 h (control without treatment), 2 h and 4 h. For each incubation time, 2 ml of SC-AgNPs (MIC and 1/2 MIC) were added to 8 ml bacteria cultured at their logarithm growth phase ($1 \times 10^8$ CFU/mL) and incubated at 37 °C. After the incubation period, bacterial culture was collected and centrifuged to collect bacterial pellets. These bacterial pellets were fixed in 2% glutaraldehyde solution for 24h at 4 °C. After fixation, the cubes were washed with PBS solution followed by the dehydration process by immersing the pallet in a gradual

concentration of ethanol ranging from 10 to 100% for 15 min. Samples were dried in $CO_2$ using the critical point method. Next, the dried samples were mounted onto a stub and coated with a thin layer of gold and viewed under SEM (Carl Zeiss Leo 1450VP, United Kingdom).

### Gene expression analysis

#### RNA extraction

RNA isolation was isolated by using the Innuprep RNA Mini Isolation kit (Analytik Jena, Jerman). RNA isolation had been done on *S. mutans, E. coli and P. aeruginosa* treated with SC-AgNPs (MIC and ½ MIC) and non-treated bacteria. Following purification, the RNA concentration was measured by using NanoDrop 2000c spectrophotometer (Thermo Fisher Scientific, Waltham, MA, USA). Ratios of A260/A280 and A260/A230 were measured to confirm the RNA isolations were free from contaminants.

#### Real-time PCR

Real-time PCR analysis was done by using SensiFAST™ SYBR® No-ROX One-Step Kit (Bioline, UK). The primers for this analysis were *eae A* [F- GACCCGGCACAAGCATAAGC, R- CCA CCTGCAGCAACAAGAGG- [25]] for *E. coli*, *Pel* A [F-ACAGCC AGGTAATGGACCTC, R- AAGCTGTCCAGGGTATCGAG- [26]] for P. aeruginosa and *gtf* B (F-AGC AAT GCA GCC AAT CTA CAA AT, R-ACG AAC TTT GCC GTT ATT GTC-A- [27] for *S. mutans*. A real-time PCR assay was performed using CFX96 Touch Real-Time PCR Detection System. Reaction mixtures were prepared following the manufacturer's protocol. The amplification program was set at 50 °C for 10 min and 95 °C for 10 min, followed by 35 cycles at 95 °C for 15s and 60 °C for 1 min. No template RNA was used as a negative control. The normalization of gene expression was done by using 16s RNA gene references. The fold change of gene expression was calculated by using the model from Livak and Schmittgen [28]. All the samples were done in triplicate.

### Statistical analysis

Results were expressed as mean ± SD in triplicate and the differences between treated and untreated cells were determined using ANOVA. All the tests were analyzed using One-way ANOVA. A significant difference was accepted with $p < 0.05$. Statistical analysis was performed using SPSS Statistic 25.0 (SPSS Inc. Chicago IL. USA).

## Results

### Synthesis and characterization of SC-AgNPs

Upon the addition of *S. crispus* leaves water extract into the $AgNO_3$ solution, the colour of the mixture was gradually transformed to dark brown indicating the formation of SC-AgNPs [Figure 1(B)]. UV–Vis spectrometry of *S. crispus* leaves extract and SC-AgNPs are shown in Figure 2(A) and 2(B), respectively. A sharp peak around 400 nm wavelength showed the presence of AgNP in the solution after 24 h of non-stop stirring under room temperature [14]. Dynamic light scattering (DLS) was used to measure particle size of the synthesised SC-AgNPs. Table 1 summarises the results of particle size and zeta potential analysis. SC-AgNPs showed an average size distribution of 75.25 nm. The polydispersity index (PDI) for SC-AgNPs was 0.373. SC-AgNPs showed a value of −35.6 mV for the zeta potential measured. FESEM was done to determine the surface morphology of synthesized AgNPs. Based on Figure 2(C), FESEM images showed that the synthesized SC-AgNPs had rough surfaces with a spherical shape. SC-AgNPs were analyzed using XRD to determine the crystalline phase of the synthesized AgNP. Figure 2(D) shows the XRD pattern of SC-AgNPs. The main peaks for SC-AgNPs clearly appeared at ($2\theta$) 38.20 (111), 44.40 (200), 64.60 (220), 77.60 (311), and 81.76 (222) planes, indicating the face-centred cubic structures of SC-AgNPs [29]. Figure 2(E) shows the FTIR analysis comparison between *S. crispus* water extract and the SC-AgNPs. FTIR revealed a shifted peak from 1404.99 to 1345.00 $cm^{-1}$ which corresponds to C–O–H bending of carboxylic acid vibrations.

### Disc diffusion assay

The result from the disc diffusion assay showed that SC-AgNPs (10 mg/mL) exhibited greater zone inhibition against all bacteria compared to AgNP blank and *S. crispus* water extract. Table 2 presented the results of zone inhibition after being treated with SC-AgNPs, AgNP blank and *S. crispus* water extract. *S. mutans* was resistant to *S. crispus* water extract and AgNP blank. The zone inhibition values of SC-AgNPs against all the bacteria showed a significant difference ($p < 0.05$) when compared to AgNP blank and *S. crispus* water extract.

### MIC And MBC

The MIC value of SC-AgNPs against *E. coli, P. aeruginosa* and *S. mutans* were 1.25, 1.25 and 2.5 mg/mL of concentrations, respectively (Table 3). The MBC values of SC-AgNPs against all the bacteria were 2.5 mg/mL of concentration. Meanwhile, MIC and MBC values of AgNP blank against *E. coli* and *P. aeruginosa* were 10 mg/mL of concentration, respectively. The MIC and MBC values of AgNP blank and *S. crispus* water extract against *S. mutans* were more than 10 mg/mL respectively. The MIC and MBC values of SC-AgNPs against the bacteria were significantly different ($p < 0.05$) when compared to AgNP blank and *S. crispus* water extract. SC-AgNPs exhibited the lowest concentrations of MIC and MBC values against all the bacteria when compared with AgNP blank and *S. crispus* water extract. However, a significant difference ($p < 0.05$) in MIC and MBC values was shown between SC-AgNPs and gentamicin.

### Time kill assay

In time-kill analysis, *P. aeruginosa* growth was significantly reduced ($p < 0.05$) by more than $>$ 3 $\log_{10}$ CFU/mL after being treated with SC-AgNPs (0.625–2.5 mg/mL) at 4, 8, 12

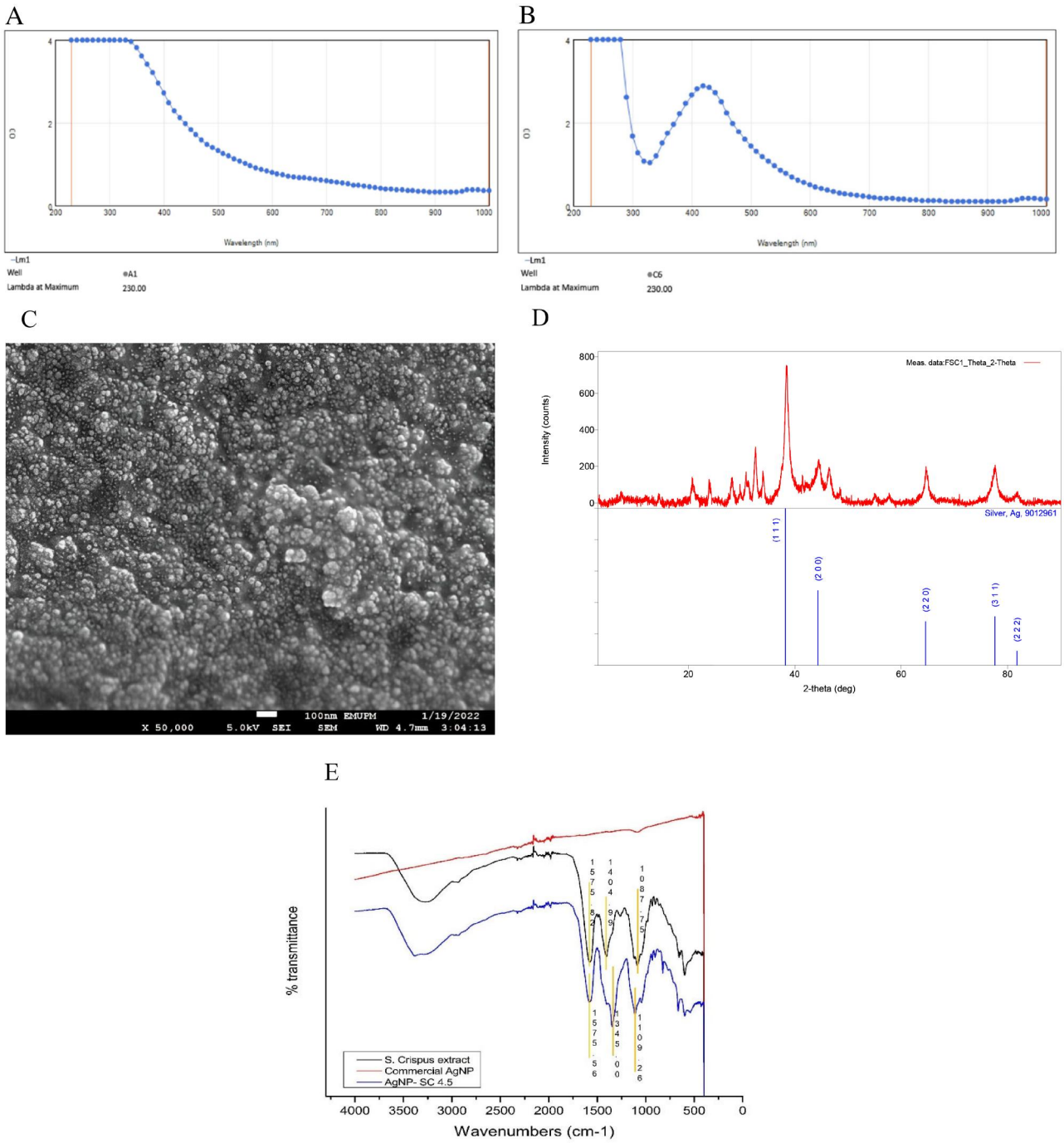


**Figure 2.** Characterization of SC-AgNPs. (A) UV-Vis spectra of *S. crispus* leaves water extract at 4.5 mg/mL; (B): UV-Vis spectra of SC-AgNPs at 4.5 mg/mL; (C) FESEM images of SC-AgNPS at 50,000 × magnification; (D) XRD spectra of SC-AgNPs; (E) FTIR analysis of commercial AgNPs, *S. crispus* aqueous extract and SC-AgNPs.

**Table 1.** Particle size and zeta potential analysis.

| Polydispersity index (PDI) | Particle size (nm) | Zeta potential (mV) |
|---|---|---|
| 0.373 | 75.25 | −35.6 |

and 24 h [Figure 3(A)] when compared to non-treated bacteria (control) ($p < 0.05$). *E. coli* was significantly reduced to more than >3 $\log_{10}$ CFU/mL after being treated with SC-AgNPs (1.25–2.5 mg/mL) [Figure 3(B)]. However, SC-AgNPs (0.625 mg/mL) significantly reduced less than <3 $\log_{10}$ Cfu/mL of bacteria growth after 4 h of treatment ($p < 0.05$). On the other hand, *S. mutans* was reduced to less than <3 $\log_{10}$ CFU/mL after being treated with SC-AgNPs (1.25 and

**Table 2.** Zone inhibition of bacteria after exposure to SC-AgNPs, AgNP, *S. crispus* water extract and gentamicin.

| | Zone inhibition (mm) | | |
|---|---|---|---|
| Samples (mg/mL) | *E. Coli* | *P. aeruginosa* | *S. mutans* |
| SC-AgNPs (10) | $12.5 \pm 0.87^{b}$ | $12.71 \pm 0.87^{b}$ | $11.00 \pm 0.33^{b}$ |
| AgNP (10) | $7.3 \pm 0.58^{a}$ | $7.9 \pm 0.32^{a}$ | $6.0 \pm 0.00^{a}$ |
| *S. crispus* (10) | $6.0 \pm 0.00^{a}$ | $6.0 \pm 0.00^{a}$ | $6.0 \pm 0.00^{a}$ |
| Gentamicin (10 µg) | $23.5 \pm 0.7^{c}$ | $20.1 \pm 0.22^{c}$ | $40.0 \pm 0.06^{c}$ |

The concentration of SC-AgNPs, AgNP and *S. crispus* water extract against *E. coli*, *S. mutans* and *P. aeruginosa* were 10 mg/mL, respectively. AgNP incorporated with *S. crispus* exhibited greater zone inhibition against bacteria compared to blank AgNP and *S. crispus* water extract. Samples were analysed in triplicate and data were presented as means ± standard deviation. Mean values within a row with different letters (a–c) were significantly different ($p < 0.05$). the zone diameter of 6.0 ± 0.00 mm was presented as no inhibition activity.

0.625 mg/mL) at 24 h of treatment when compared to the control [Figure 3(C)]. Whereas *S. mutans* growth was significantly reduced by more than >3 $\log_{10}$ CFU/mL after being treated with 2.5 mg/mL (MBC) of SC-AgNPs after 24 h of treatment compared to the control ($p < 0.05$).

This analysis also showed that AgNP blank (MIC:10 mg/mL) reduced ($p < 0.05$) *P. aeruginosa* and *E. coli* growth by more than >3 $\log_{10}$ CFU/mL at 4, 8, 12 and 24 h when compared to control [Figure 3(A,B)]. However, AgNP blank reduced less than <3 $\log_{10}$ CFU/mL of *S. mutans* growth after 24 h of treatment [Figure 3(C)]. No significant reducing pattern of *P. aeruginosa*, *S. mutans* and *E. coli* growth after being treated with *S. crispus* water extract (10 mg/mL) when compared to control ($p > 0.05$). Gentamicin (MIC) significantly reduced *P. aeruginosa* and *S. mutans* growth by more than >3 $\log_{10}$ CFU/mL at 4, 8, 12 and 24 h when compared to the control ($p < 0.05$). Meanwhile, *E. coli* growth was reduced by more than >3 $\log_{10}$ CFU/mL with gentamicin (MIC) at 12 and 24 h of treatment.

## Scanning electron microscope (SEM)

The morphologies of *E. coli* and *P. aeruginosa* treated with SC-AgNPs were different when compared to the control. The morphology of non-treated bacteria for *E. coli* was observed as rod and chain [Figure 4(A)]. Meanwhile, morphologies of *E. coli* treated with SC-AgNPs (0.625 and 1.25 mg/mL) were found shrunken and irregular in shape [Figure 4(B,C)]. Non-treated *P. aeruginosa* was rods in shape and clustered [Figure 5(A)]. Meanwhile, *P. aeruginosa* treated with SC-AgNPs (0.625 and 1.25 mg/mL) was observed to be shrunken [Figure 5(B)] and lysed [Figure 5(C)]. The morphology of *S. mutans* treated with SC-AgNPs (1.25 and 2.5 mg/mL) at 4 h does not change much compared to non-treated bacteria. The morphology of non-treated *S. mutans* was coccus and chain [Figure 6(A)]. Meanwhile, the size of certain treated *S. mutans* was found smaller and irregular in shape [Figure 6(B,C)].

**Table 3.** MIC and MBC of SC-AgNPs, AgNP and *S. crispus* water extract against *E. coli, P. aeruginosa* and *S. mutans*.

| | *E. coli* | | *P. aeruginosa* | | *S. mutans* | |
|---|---|---|---|---|---|---|
| Samples | MIC | MBC | MIC | MBC | MIC | MBC |
| SC-AgNPs (mg/mL) | 1.25 | 2.5 | 1.25 | 2.5 | 2.5 | 2.5 |
| AgNP (mg/mL) | 10.00 | 10.00 | 10.00 | 10.00 | >10.00 | >10.0 |
| *S. crispus* extract (mg/mL) | >10.00 | >10.00 | >10.00 | >10.00 | >10.00 | >10.00 |
| Gentamicin (µg/mL) | 6.25 | 12.5 | 3.13 | 6.25 | 25.00 | 25.00 |

The values of MIC and MBC for SC-AgNPs against all bacteria were lower compared to AgNP blank and *S. crispus* water extract. The sample was analyzed in triplicate and data are presented as means ± standard deviation.

## Gene expression level

Each treated bacteria (*S. mutans, P. aeruginosa and E. coli*) successfully extracted its RNA at ½ MIC and MIC. Whereas nontreated RNA for each type of bacteria was used as a control. The RNAs concentration range for all samples was 500–1500 ng/µL, respectively. The A260/280 ratio for all RNA samples was 1.9–2.0. All the RNAs were used for gene expression analysis. Differential expression genes (DEG) levels of bacteria treated with SC-AgNPs were analyzed on *eae A* gene for *E. coli*, *Pel* A gene for *P. aeruginosa* and *gtf* B gene for *S. mutans*. Figure 7(A) showed the DEG level (fold change) of *eae* A gene was significantly ($p < 0.05$) downregulated after *E. coli* was treated with SC-AgNPs at 0.625 (Fold Change: 0.18) and 1.25 mg/mL (Fold Change: 0.02) when compared to non-treated (Fold Change: 1) ($p < 0.05$). Meanwhile, the fold change of the *gtf* B gene was downregulated after *S. mutans* were treated with SC-AgNPs at 1.25 (Fold Change: 0.97) and 2.5 mg/mL (Fold Change: 0.84) when compared to non-treated (Fold Change: 1) ($p < 0.05$) [Figure 7(B)]. However, the

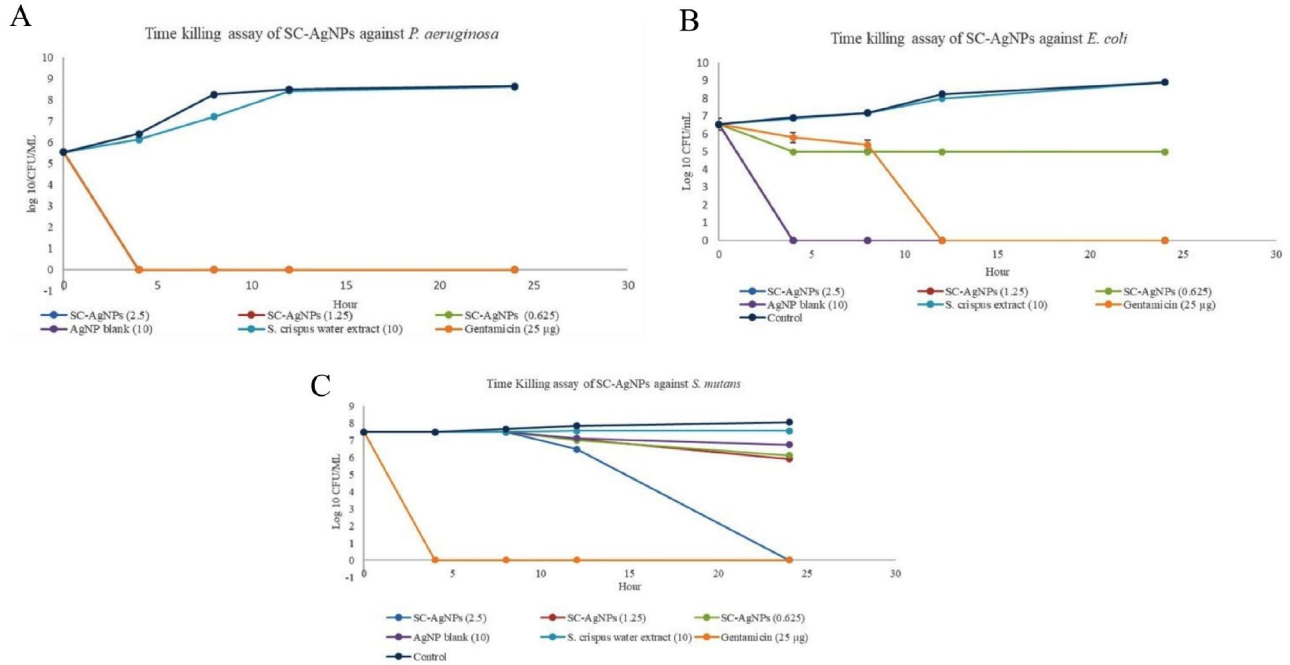


**Figure 3.** (A) the growth of *P. aeruginosa,* (B) *E. coli,* (C) *S. mutans* ($\log_{10}$ Cfu/mL) after being treated with SC-AgNPs, AgNP and *S. crispus* water extract at 0, 4, 8, 12 and 24 h. The samples were analyzed in triplicate and data were presented as means ± standard deviation.

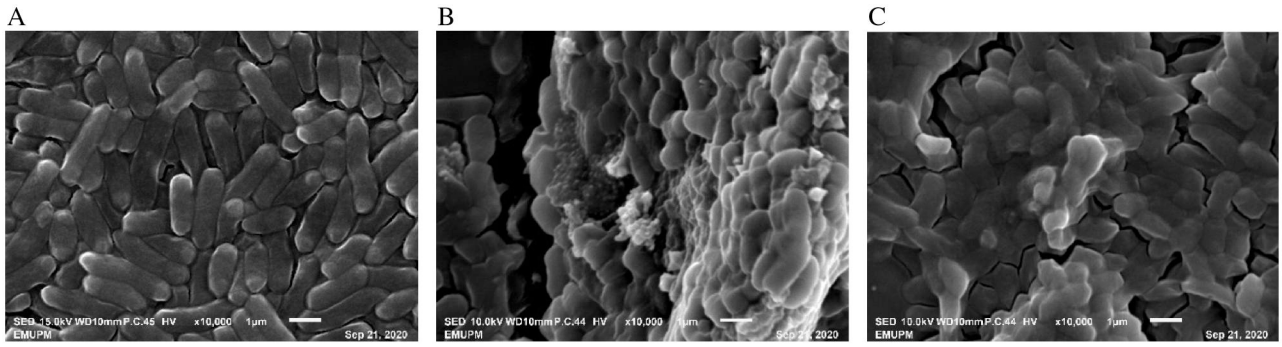


**Figure 4.** (A) Morphology of non-treated *E. coli*, (B) morphology of *E. coli* after being treated with SC-AgNPs (1.25 mg/mL) and (C) morphology of *E. coli* after being treated with SC-AgNPs (0.625 mg/mL). Non-treated *E. coli* was rod in shape, meanwhile, *E. coli* treated with SC-AgNPs was smaller, shrunken and irregular in shape.

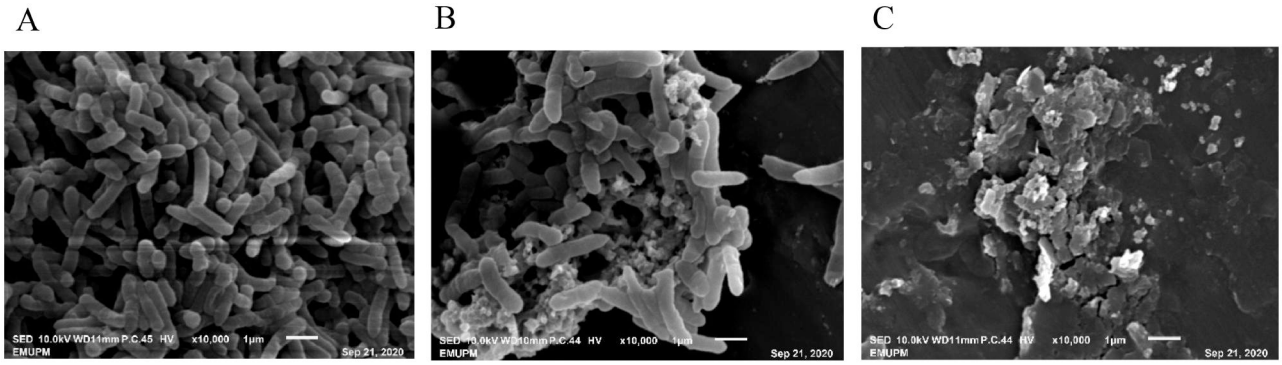


**Figure 5.** (A) Morphology of non-treated *P. aeruginosa*, (B) morphology of *P. aeruginosa* after being treated with SC-AgNPs (0.625 mg/mL) and (C) morphology of *P. aeruginosa* after being treated with SC-AgNPs (1.25 mg/mL). Non-treated *P. aeruginosa* was rod in shape, meanwhile, *P. aeruginosa* treated with SC-AgNPs was found lysed and shrunken.

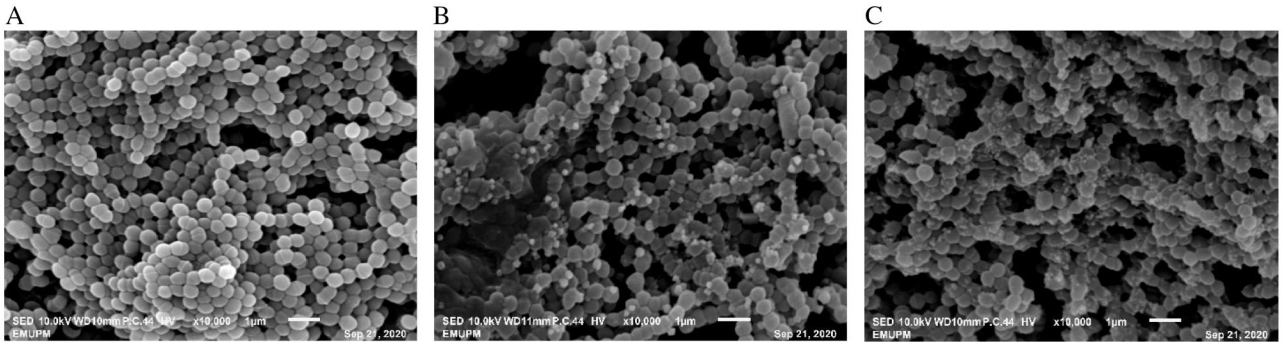


**Figure 6.** (A) Morphology of non-treated *S. mutans*, (B) morphology of *S. mutans* after being treated with SC-AgNPs (2.5 mg/mL) and (C) morphology of *S. mutans* after being treated with SC-AgNPs (1.25 mg/mL). Non-treated *S. mutans* was coccus in shape, meanwhile, *S. mutans* treated with SC-AgNPs was smaller and irregular in shape.

fold change of *Pel* A gene was significantly up-regulated ($p < 0.05$) after *P. aeruginosa* was treated with SC-AgNPs at 0.625 (Fold Change: 3.84) and 1.25 mg/mL (Fold Change: 15.14) when compared to non-treated (Fold Change: 1) [Figure 7(C)].

## Discussion

The green synthesis silver nanoparticles method has been known to offer rapid, environmentally friendly and cost-effective yield [14]. In this study, *Strobilanthes crispus* water extract was used as a reducing and capping agent. The presence of dark brown pigment in silver nitrate solution indicated the formation of silver nanoparticles. Dynamic light scattering (DLS) measured the average particle size of SC-AgNPs at 75.25 nm. The calculated PDI value of SC-AgNPs was 0.373 (Table 1) which is within the range of 0–1 where 0 refers to monodisperse and 1 is polydisperse [20]. This outcome evidently shows that the synthesized SC-AgNPs were monodisperse. SC-AgNPs developed in this study show a high degree of stability (−35.6 mV), as reported by Heydari & Rashidipour [30], a high degree of stability of nanoparticles possessing a zeta potential value of more than 25 mV or lower than −25 mV. A high negative charge (−35.6 mV) of SC-AgNPs may show a strong repulsive force between the

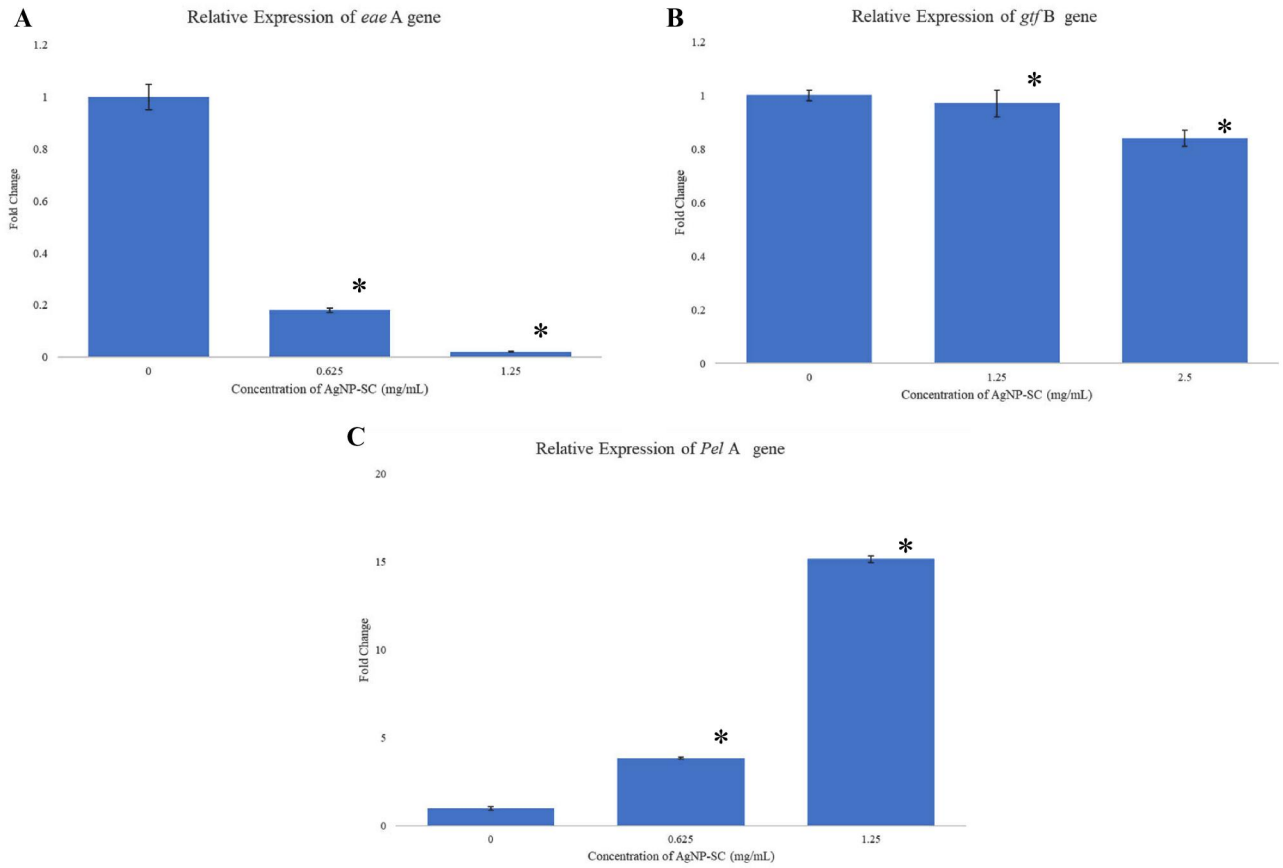


**Figure 7.** (A) The relative expression of *eae* a gene in *E. coli*, (B) *gtf* B gene in *S. mutans* and (C) *Pel* a gene in *P. aeruginosa* after being treated with SC-AgNPs. The samples were analyzed in triplicate and data were presented as means ± standard deviation. The fold change value of treated genes showed significant differences ($p < 0.05$) when compared to control (*).

particles which prevents particle aggregation. On the other hand, the surface morphology of synthesized SC-AgNPs showed that the synthesized SC-AgNPs had rough surfaces with a spherical shape [Figure 2(C)]. This result was in concordance with PDI and zeta values data which stated SC-AgNPs were monodisperse with minimal aggregation. Meanwhile, XRD analysis identified silver in the synthesized sample by comparing the peaks with the silver database from the Joint Committee on Powder Diffraction Standard (JCPDS) or International Centre for Diffraction Data (ICDD) [20]. These results showed that SC-AgNPs were pure crystalline and confirmed the presence of silver in the synthesized sample. FTIR analysis reported C–O–H bending of carboxylic acid vibrations when compared to *S. crispus* water extract. This indicates bioactive compounds such as stigmasterol, β-sitosterol, ferulic acid and vanillic acid [31] in *S. crispus* water extract may be responsible for reducing $Ag^{+}$ to $Ag^{0}$ in the synthesised sample.

The antibacterial assay of this study showed that SC-AgNPs were more potent when compared to AgNP blank and *S. crispus* water extract. In the disc diffusion assay, SC-AgNPs exhibited greater zone inhibition against all bacteria compared to AgNP blank and *S. crispus* water extract. Meanwhile, the MIC and MBC values of SC-AgNPs were the lowest concentration against *S. mutans*, *E. coli* and *P. aeruginosa* when compared to other samples. Minimum inhibitory concentration (MIC) is defined as the lowest concentration of an antimicrobial that will inhibit the visible growth of a microorganism after overnight incubation, and minimum bactericidal concentrations (MBCs) as the lowest concentration of an antimicrobial that will prevent the growth of an organism after subculture onto antibiotic-free media [32]. In this study, MIC and MBC values of SC-AgNPs were the lowest when compared to AgNP blank and *S. crispus* water extract. This analysis showed that SC-AgNPs enhanced its medicinal properties against bacteria. According to Park [33], AgNP will increase the surface area to volume ratios of plant extraction. The larger surface area will provide many opportunities for interaction between extract and tested bacteria. Thus, a low concentration of samples is favoured to be deemed as effective as an antibacterial agent. Hence, SC-AgNPs have shown to inhibit or kill the growth of *E. coli*, *P. aeruginosa* and *S. mutans* at low concentrations (0.625 mg/mL)

An antibacterial agent is defined as bactericidal if it decreases the colony by more than $> 3$ $\log_{10}$ Cfu/mL, which is equivalent to 99.9% killing of bacteria (Hanafiah et al. 2015). The rate of killing time assay showed that *P. aeruginosa* and *E. coli* growths reduced more than $>3$ $\log_{10}$ Cfu/mL after being exposed to SC-AgNPs at 0.625, 1.25 and 2.5 mg/mL concentrations. Meanwhile, AgNP blank (10 mg/mL) reduced *P. aeruginosa* and *E. coli* growth by more than $>3$ $\log_{10}$ Cfu/mL. However, the rate killing time of bacteria treated with *S. crispus* water extract (10 mg/mL) showed no growth reduction in *P. aeruginosa*, *S. mutans* and *E. coli*. This

finding showed that incorporation between AgNP and plant extract (*S. crispus* water extract) produces smaller AgNP which then increases the surface area to provide more interaction opportunities with bacteria so that a lower concentration of SC-AgNPs will be effective as a bactericidal agent. A previous study by Dar et al. [34] also showed that AgNP incorporates with biological extracts (metabolite from *Cryphonectria* sp) enhanced the activities of common antibiotics. AgNPs were used to preserve water and help to inhibit bacteria by interrupting the DNA of bacteria function [35]. AgNP has different antibacterial properties depending on its scale and size. The largest surface area of AgNP gives the best effects in antibacterial activities [35]. According to Morones et al. [37], AgNP with a size of 10–100 nm showed strong antimicrobial activities against pathogenic bacteria. The incorporation of AgNP with plant extraction is the eco-friendly route for the synthesis process and at the same time enhances their antimicrobial activities. To the best of our knowledge, the present study is the first to report incorporation between AgNP and *S. crispus* water extract enhanced their antibacterial properties against *S. mutans, P. aeruginosa and E. coli*.

The morphological analysis had been done on treated bacteria to observe their changes with non-treated bacteria. From the present study, the concentration of SC-AgNPs was the lowest among all bacteria as compared to AgNP blank and *S. crispus* water extract. The MIC value of SC-AgNPs against *E. coli, P. aeruginosa* and *S. mutans* were 1.25, 1.25 and 2.5 mg/mL of concentrations, respectively (Table 2). The morphological analysis used MIC (1.25, 1.25 and 2.5 mg/mL) and $^1/_2$ MIC (0.625 and 1.25 mg/mL) concentrations for each treated bacteria, respectively. Morphologies of *P. aeruginosa* and *E. coli* after being treated with SC-AgNPs were different when compared to non-treated bacteria. SEM analysis confirmed the results from the time-kill assay that both bacteria were found dead after 4 h of treatment with SC-AgNPs. The particle of SC-AgNPs was adhered to the cell wall and then penetrated and lysis the cell [13]. Other than that, AgNP will help penetrate the bacterial cell wall, increase cell permeability and subsequently followed by cell death.

The morphology of *S. mutans* treated with SC-AgNPs was shown as smaller and irregular in shape when compared to non-treated bacteria. However, the difference is not as obvious as in other bacteria due to the thickness of the cell wall of *S. mutans*. *S. mutans* is a Gram-positive bacterium, with thicker peptidoglycan compared to Gram-negative bacteria such as *E. coli and P. aeruginosa* [38]. SEM analysis of *S. mutans* was in concordance with the result from the time-kill assay that the bacteria was not dead after 4 h of treatment. However, they were found dead after 24 h of treatment when treated with SC-AgNPs (2.5 mg/mL).

In gene expression analysis, SC-AgNPs interrupted the function of the gene involved in adherence and biofilm activities of those bacteria. *eae* A gene encoded protein intimin. It is responsible for attachment interaction between *E. coli* and the host. Intimin binds to the cell receptor Tir, which is translocated by the pathogen to the enterocyte via a type III secretion system and is responsible to attach on the epithelial cells of the host [39]. The *eae* A gene of *E. coli* was downregulated after being treated with SC-AgNPs at 0.625 and 1.25 mg/mL concentrations. According to Mei et al. [40], *eae* A gene of *E. coli* O26:H11 was significantly ($p < 0.05$) downregulated after being exposed to hydrogen peroxide. This analysis suggested that the down-regulated of *eae* A gene may inhibit the attachment activities of *E. coli*.

The attachment of *S. mutans* is dependent on the production of glucan polymers from sucrose enhanced by the glucosyltransferase enzyme. Glucosyltransferase enzymes are encoded by *gtf* gene. The Gene of *gtf* B is an exoenzyme involved with the extracellular metabolism of sucrose and synthesize a polymer synthesizes a polymer of insoluble ($\alpha$-1,3-linked) glucan [41]. These glucans are important components of the matrix of cariogenic biofilms. In this study, *gtf* B gene was downregulated after being treated with SC-AgNPs at 1.25 and 2.5 mg/mL concentrations. Interruption of this gene may inhibit the formation of biofilm in *S. mutans*. A previous study found that the *gtf* B gene was downregulated and effectively reduced *S. mutans* adherence after being exposed to hydroxy-decanoic acid.

The Pel A gene encodes the extracellular polymeric substance (EPS) of *P. aeruginosa*. Pel polysaccharides are glucose-rich and can promote irreversible attachment [42]. Pel polysaccharides serve as structural components of the biofilm matrix [42]. Regulation of Pel polysaccharide involves 3,5-cyclic diguanylic acid (c-di-GMP) which is formed by diguanylate cyclases with GGDEF motifs. Many proteins with GGDEF motifs enhance the biofilm formation of *P. aeruginosa* [44]. A previous study found that C-di-GMP upregulated after *P. aeruginosa* responds to tellurite during biofilm modes of growth [45]. In this study, *Pel* A genes were upregulated after being treated with SC-AgNPs (0.625 and 1.25 mg/mL). *Pel* A gene plays an important role in surface attachment and biofilm formation of *P. aeruginosa*. Interruption of this gene may inhibit the formation of biofilm in *P. aeruginosa*.

## Conclusions

SC-AgNPs exhibited greater antibacterial activities against *S. mutans, P. aeruginosa and E. coli* compared to AgNP blank and *S. crispus* water extract. The antibacterial assay of this study showed that SC-AgNPs was more potent when compared to AgNP blank and *S. crispus* water extract. In the disc diffusion assay, SC-AgNPs exhibited greater zone inhibition against all bacteria compared to AgNP blank and *S. crispus* water extract. Meanwhile, the MIC and MBC values of SC-AgNPs were the lowest concentration against *S. mutans*, *E. coli* and *P. aeruginosa* when compared to other samples. It also altered all the bacteria morphologies from their original form to be lysed and shrunk. Besides that, SC-AgNPs disrupted the gene expression of *eae* A, *gtf* B and *Pel* A which are responsible for the attachment and biofilm formation activities of bacteria. The findings were in a dose-dependent manner, with higher concentrations showing better inhibition activities. The future of synthesizing silver nanoparticles using *S. crispus* is full of exciting possibilities across various domains, including healthcare such as antibacterial agents and agriculture. The continued exploration of this field has

the potential to yield innovative solutions that address some of the pressing challenges faced by society while aligning with sustainable, healthy and environmentally friendly practices.

## Author contributions

SAAG, RMH and SNAM contributed to the design, interpreted the data and manuscript writing. Meanwhile, VL, YF & AHHA contributed to the synthesis of SC-AgNPs.

## Disclosure statement

No potential conflict of interest was reported by the author(s).

## Funding

This research was funded by the Fundamental Research Grant Scheme (FRGS) of the Ministry of Higher Education (MOHE), Malaysia (FRGS/1/2021/STG05/USIM/02/2).

## ORCID

Rohazila Mohamad Hanafiah http://orcid.org/0000-0002-7180-0967
Siti Aisyah Abd Ghafar http://orcid.org/0000-0002-7680-0130

## Data availability statement

The data are available from the corresponding author upon reasonable request. The whole methodology is included in the materials and methods section.

## References

[1] Sharif MS, Hameed H, Waheed A, et al. Biofabrication of $Fe_3O_4$ nanoparticles from *spirogyra hyalina* and *ajuga bracteosa* and their antibacterial applications. Molecules. 2023;28(8):3403. doi: 10.3390/molecules28083403.

[2] Hao P, Li H, Zhou L, et al. Serum metal ion-induced cross-linking of photoelectrochemical peptides and circulating proteins for evaluating cardiac ischemia/reperfusion. ACS Sens. 2022;7(3):775–783. doi: 10.1021/acssensors.1c02305.

[3] Harish V, Tewari D, Gaur M, et al. Review on nanoparticles and nanostructured materials: bioimaging, biosensing, drug delivery, tissue engineering, antimicrobial, and agro-food applications. Nanomaterials. 2022;12(3):457. 2022 doi: 10.3390/nano12030457.

[4] Saqib S, Faryad S, Afridi MI, et al. Bimetallic assembled silver nanoparticles impregnated in aspergillus fumigatus extract damage the bacterial membrane surface and release cellular contents. Coatings. 2022;12(10):1505–1515. doi: 10.3390/coatings12101505.

[5] Burdușel AC, Gherasim O, Grumezescu AM, et al. Biomedical applications of silver nanoparticles: an up-to-date overview. Nanomaterials. 2018;8(9):681. doi: 10.3390/nano8090681.

[6] Ahmed S, Ahmad M, Swami BL, et al. A review on plants extract mediated synthesis of silver nanoparticles for antimicrobial applications: a green expertise. J Adv Res. 2016;7(1):17–28. doi: 10.1016/j.jare.2015.02.007.

[7] Hano C, Abbasi BH. Plant-Based green synthesis of nanoparticles: production, characterization and applications. Biomolecules. 2021;12(1):31. doi: 10.3390/biom12010031

[8] Verma A, Mehata MS. Controllable synthesis of silver nanoparticles using neem leaves and their antimicrobial activity. J Radiat Res Appl Sci. 2016;9(1):109–115. doi: 10.1016/j.jrras.2015.11.001.

[9] Kumar D, Kumar G, Agrawal V. Green synthesis of silver nanoparticles using *holarrhena antidysenterica* (L.) wall. bark extract and their larvicidal activity against dengue and filariasis vectors. Parasitol Res. 2018;117(2):377–389. doi: 10.1007/s00436-017-5711-8.

[10] Kumar D, Kumar G, Das R, et al. Strong larvicidal potential of silver nanoparticles (AgNPs) synthesized using *holarrhena antidysenterica* (L.) wall. Bark extract against malarial vector, *Anopheles stephensi* liston. Process Safety and Environmental Protection. 2018;116:137–148. doi: 10.1016/j.psep.2018.02.001.

[11] Yadav R, Saini H, Kumar D, et al. Bioengineering of *Piper longum* L. extract mediated silver nanoparticles and their potential biomedical applications. Mater Sci Eng C Mater Biol Appl. 2019;104:109984. doi: 10.1016/j.msec.2019.109984.

[12] Nindawat S, Agrawal V. Fabrication of silver nanoparticles using *Arnebia hispidissima* (lehm.) A. DC. root extract and unravelling their potential biomedical applications. Artif Cells Nanomed Biotechnol. 2019;47(1):166–180. doi: 10.1080/21691401.2018.1548469.

[13] Paredes D, Ortiz C, Torres R. Synthesis, characterization, and evaluation of antibacterial effect of Ag nanoparticles against *Escherichia coli* O157: h 7 and *methicillin-resistant Staphylococcus aureus* (MRSA). Int J Nanomedicine. 2014;9:1717–1729. doi: 10.2147/IJN.S57156.

[14] Yakop F, Abd Ghafar SA, Yong YK, et al. Silver nanoparticles *clinacanthus nutans* leaves extract induced apoptosis towards oral squamous cell carcinoma cell lines. Artif Cells Nanomed Biotechnol. 2018;46(sup2):131–139. doi: 10.1080/21691401.2018.1452750.

[15] Panpaliya NP, Dahake PT, Kale YJ, et al. In vitro evaluation of antimicrobial property of silver nanoparticles and chlorhexidine against five different oral pathogenic bacteria. Saudi Dent J. 2019;31(1):76–83. doi: 10.1016/j.sdentj.2018.10.004.

[16] Lasano NF, Rahmat A, Ramli NS, et al. Effect of oven and microwave drying on polyphenols content and antioxidant capacity of herbal tea from *Strobilanthes crispus* leaves. Asian J Pharm Clin Res. 2018;11(6):363–368. doi: 10.22159/ajpcr.2018.v11i6.24660.

[17] Koay YC, Wong KC, Osman H, et al. Chemical constituents and biological activities of *Strobilanthes crispus* L. Rec Nat Prod. 2013;7(1):59–64.

[18] Lim V, Yap CS, Chong HW, et al. Antimicrobial evaluation and GC-MS analysis of *Strobilanthes crispus* ethanolic leaf extract. Methodology. 2013;10:1–8

[19] Yakop F, Abd Ghafar SA, Hanafiah RM, et al. Synthesis, characterization and cytotoxicity of silver Nanoparticles-Strobilanthes crispus (AgNp-SC) against breast cancer cell line (MCF-7). Postgraduate Research Symposium 2022, Faculty of Dentistry USIM; 2022. p. 29.

[20] Mat Yusuf SNA, Che Mood CNA, Ahmad NH, et al. Optimization of biogenic synthesis of silver nanoparticles from flavonoid-rich *Clinacanthus nutans* leaf and stem aqueous extracts. R Soc Open Sci. 2020;7(7):200065. doi: 10.1098/rsos.200065.

[21] Salehuddin NSB, Hanafiah RBM, Ghafar SAA. Antibacterial activity of *acmella paniculata* extracts against *Streptococcus mutans*. Int J Res Pharm Sci. 2020;11(4):5735–5740.

[22] Lu J, Chen Y, Ding M, et al. A 4arm-PEG macromolecule crosslinked chitosan hydrogels as antibacterial wound dressing. Carbohydr Polym. 2022;277:118871. doi: 10.1016/j.carbpol.2021.118871.

[23] Hanafiah RM, Aqma WS, Yaacob WA, et al. Antibacterial and biofilm inhibition activities of Melastoma malabathricum stem bark extract against Streptococcus mutans. Malaysian Journal of Microbiology. 2015;11(2):199–206.

[24] Goldbeck JC, Victoria FN., Motta A, et al. Bioactivity and morphological changes of bacterial cells after exposure to 3-(p-chlorophenyl) thio citronellal. LWT-Food Science and Technology, 2014;59(2):813–819.

[25] Abreham S, Teklu A, Cox E, et al. *Escherichia coli* O157: h 7: distribution, molecular characterization, antimicrobial resistance patterns and source of contamination of sheep and goat carcasses at an export Abattoir, Mojdo, Ethiopia. BMC Microbiol. 2019;19(1):215. doi: 10.1186/s12866-019-1590-8.

[26] She P, Wang Y, Liu Y, et al. Effects of exogenous glucose on *Pseudomonas aeruginosa* biofilm formation and antibiotic resistance. Microbiologyopen. 2019;8(12):e933. doi: 10.1002/mbo3.933.

[27] Veloz JJ, Saavedra N, Alvear M, et al. Polyphenol-rich extract from propolis reduces the expression and activity of *Streptococcus mutans* glucosyltransferases at subinhibitory concentrations. Biomed Res Int. 2016;2016:4302706–4302707. doi: 10.1155/2016/4302706.

[28] Livak KJ, Schmittgen TD. Analysis of relative gene expression data using real-time quantitative PCR and the 2− ΔΔCT method. Methods. 2001;25(4):402–408. doi: 10.1006/meth.2001.1262.

[29] Deng SP, Zhang JY, Ma ZW, et al. Facile synthesis of long-term stable silver nanoparticles by kaempferol and their enhanced antibacterial activity against *Escherichia coli* and *Staphylococcus aureus*. J Inorg Organomet Polym. 2021;31(7):2766–2778. doi: 10.1007/s10904-020-01874-2.

[30] Heydari R, Rashidipour M. Green synthesis of silver nanoparticles using extract of oak fruit hull (jaft): synthesis and *in vitro* cytotoxic effect on MCF-7 cells. Int J Breast Cancer. 2015;2015(846743):846743–846746. doi: 10.1155/2015/846743.

[31] Nurraihana H, Norfarizan-Hanoon NA. Phytochemistry, pharmacology and toxicology properties of *Strobilanthes crispus*. Int Food Res J. 2013;20(5):2045.

[32] Andrews JM. Determination of minimum inhibitory concentrations. J Antimicrob Chemother. 2001;48(suppl_1):5–16. doi: 10.1093/jac/48.suppl_1.5.

[33] Park Y. A new paradigm shift for the green synthesis of antibacterial silver nanoparticles utilizing plant extracts. Toxicol Res. 2014;30(3):169–178. doi: 10.5487/TR.2014.30.3.169.

[34] Dar MA, Ingle A, Rai M. Enhanced antimicrobial activity of silver nanoparticles synthesized by cryphonectria sp. evaluated singly and in combination with antibiotics. Nanomedicine. 2013;9(1):105–110. doi: 10.1016/j.nano.2012.04.007.

[35] Nath D, Banerjee P. Green nanotechnology–a new hope for medical biology. Environ Toxicol Pharmacol. 2013;36(3):997–1014. doi: 10.1016/j.etap.2013.09.002.

[36] Akhtar MS, Panwar J, Yun YS. Biogenic synthesis of metallic nanoparticles by plant extracts. ACS Sustainable Chem Eng. 2013;1(6):591–602. doi: 10.1021/sc300118u.

[37] Morones JR, Elechiguerra JL, Camacho A, et al. The bactericidal effect of silver nanoparticles. Nanotechnology. 2005;16(10):2346–2353. doi: 10.1088/0957-4484/16/10/059.

[38] Pal S, Tak YK, Song JM. Does the antibacterial activity of silver nanoparticles depend on the shape of the nanoparticle? A study of the gram-negative bacterium *Escherichia coli*. Appl Environ Microbiol. 2007;73(6):1712–1720. doi: 10.1128/AEM.02218-06.

[39] Yang X, Sun H, Fan R, et al. Genetic diversity of the intimin gene (eae) in non-O157 Shiga toxin-producing *Escherichia coli* strains in China. Sci Rep. 2020;10(1):1–9.

[40] Mei GY, Tang J, Bach S, et al. Changes in gene transcription induced by hydrogen peroxide treatment of verotoxin-producing *Escherichia coli* O157: h 7 and non-O157 serotypes on romaine lettuce. Front Microbiol. 2017;8:477. doi: 10.3389/fmicb.2017.00477.

[41] Klein MI, DeBaz L, Agidi S, et al. Dynamics of Streptococcus mutans transcriptome in response to starch and sucrose during biofilm development. PLOS One. 2010;5(10):e13478. doi: 10.1371/journal.pone.0013478.

[42] Colvin KM, Irie Y, Tart CS, et al. The pel and psl polysaccharides provide *Pseudomonas aeruginosa* structural redundancy within the biofilm matrix. Environ Microbiol. 2012;14(8):1913–1928. doi: 10.1111/j.1462-2920.2011.02657.x.

[43] Jennings LK, Storek KM, Ledvina HE, et al. Pel is a cationic exopolysaccharide that cross-links extracellular DNA in the *Pseudomonas aeruginosa* biofilm matrix. Proc Natl Acad Sci USA. 2015;112(36):11353–11358. doi: 10.1073/pnas.1503058112.

[44] Ueda A, Wood TK. Connecting quorum sensing, c-di-GMP, pel polysaccharide, and biofilm formation in *Pseudomonas aeruginosa* through tyrosine phosphatase TpbA (PA3885). PLOS Pathog. 2009;5(6):e1000483. doi: 10.1371/journal.ppat.1000483.

[45] Chua SL, Sivakumar K, Rybtke M, et al. C-di-GMP regulates Pseudomonas aeruginosa stress response to tellurite during both planktonic and biofilm modes of growth. Sci Rep. 2015;5(1):10052. doi: 10.1038/srep10052.